

# Inverstigation the $\gamma P \rightarrow K^+ K^- P$ process with $B_5$ model

Meng Shi

February 8, 2014

## 1 B4 model(Nov 14 ,2013)

To illustrate the B5 model, we will begin with the G. Veneziano's Narrow resonance model[1], which is also called  $B_4$  model. In 1968, G. Veneziano was the first one wrote down the Regge behavior amplitude for  $\pi\omega \rightarrow \pi\pi$  with a Beta function,

$$\begin{aligned} T &= \varepsilon_{\mu\nu\rho\sigma} \epsilon_\omega^\mu p_1^\nu p_2^\rho p_3^\sigma \cdot A(s, t, u), \\ A(s, t, u) &= \frac{\beta}{\pi} [B(1 - \alpha(t), 1 - \alpha(s)) + B(1 - \alpha(t), 1 - \alpha(u)) + B(1 - \alpha(s), 1 - \alpha(u))], \\ B(x, y) &= \frac{\Gamma(x)\Gamma(y)}{\Gamma(x+y)}, \end{aligned} \tag{1}$$

where  $\beta$  is a constant.

The amplitude can be written,

$$\begin{aligned} A(s, t, u) &= \frac{\beta}{\Gamma(\alpha(t))\sin(\pi\alpha(t))} \frac{\sin(\pi(\alpha(s) + \alpha(t)))}{\sin(\pi\alpha(s))} \frac{\Gamma(\alpha(s) + \alpha(t) - 1)}{\Gamma(\alpha(s))} + \dots, \\ &\sim \frac{\beta(t)}{\sin(\pi\alpha(t))} \frac{1 - \cos(\pi(\alpha(t)))}{\sin(\pi\alpha(s))} [\alpha(s)]^{\alpha(t)-1}, \end{aligned} \tag{2}$$

where  $\beta(t) = \frac{\beta}{\Gamma(\alpha(t))}$ . When  $s \rightarrow \infty$ , it has  $A \propto (\alpha(s))^{\alpha(t)-1}$ , which is the Regge behavior.

The Amplitude has following properties:

- 1, Regge Behavior
- 2, Crossing symmetries
- 3, Infinity number of poles
- 4, Duality
- 5, Ploynimial residues

6, positive widths (only B4 model was proved)

7, Violation the unitarity.

Consequently, Lovelace[2] applied it to  $\pi^+\pi^-$  elastic scattering. The amplitude was written with

$$A(s, t) = -\beta \frac{\Gamma(1 - \alpha(s))\Gamma(1 - \alpha(t))}{\Gamma(1 - \alpha(s) - \alpha(t))} + \gamma \frac{\Gamma(1 - \alpha(s))\Gamma(1 - \alpha(t))}{\Gamma(2 - \alpha(s) - \alpha(t))}, \quad (3)$$

and for the isospin amplitudes

$$\begin{aligned} A^0 &= \frac{3}{2}[A(s, t) + A(s, u)] - \frac{1}{2}A(t, u), \\ A^1 &= A(s, t) - A(s, u), \\ A^2 &= A(t, u). \end{aligned} \quad (4)$$

For  $\rho$  trajectory, an imaginary part was considered

$$\alpha_\rho = 0.483 + 0.885s + i0.28\sqrt{s - 4m_\pi^2}. \quad (5)$$

The scattering length was given by this amplitude

$$a_0 = 0.395\beta, \quad a_2 = -0.103\beta. \quad (6)$$

The ratio was comparable with Weinberg's value. For  $3-\pi$  final states, such as  $\bar{p}n \rightarrow \pi^\pm\pi^\mp\pi^-$ , the amplitude were

$$\begin{aligned} \mathcal{A}(X^\pm \rightarrow \pi^\pm\pi^\pm\pi^\mp) &= A(s, t), \\ \mathcal{A}(X^\pm \rightarrow \pi^\pm\pi^0\pi^0) &= \mathcal{A}(X^0 \rightarrow \pi^+\pi^-\pi^0) = A(t, u) - A(s, t) - A(s, u), \\ \mathcal{A}(X^0 \rightarrow 3\pi^0) &= A(s, t) + A(s, u) + A(t, u). \end{aligned} \quad (7)$$

The Dalitz Plot was also fit well with this amplitude. Shapiro[3] had proved all the widths are positive. In Ref. [4], a dual model with back ground was used,

$$A(s, t) = \sum_{n,m} C_{nm} \frac{\Gamma(n - \alpha_s)\Gamma(m - \alpha_t)}{\Gamma(n + m - \alpha_s - \alpha_t)}, \quad (8)$$

$n, m = 1, 2$  and an additional term  $C_{30}$ . This amplitude can be also consist of the  $\bar{p}n \rightarrow \pi^+\pi^-\pi^-$  data including the angular distribution of  $\pi\pi$ .

About the duality—A sum of poles in one channel diverge to produce poles in overlapping channels, we will not explain it here clearly which can be viewed in the section II. D in the Ref. [5].

## 2 $B_5$ model(Nov 15 ,2013)

### 2.1 Two ways of extending the $B_4$ to $B_5$

Several authors has generalized the  $B_4$  model to the  $B_n$  model. However, they are mainly based on two different ways. One is from Ruegg[6], and the other is based on Hopkinson[8].

#### 2.1.1 Ruegg's $B_5$ model

The Ruegg amplitude is a direct generalization of  $B_4$  model to  $B_n$  model.

$$B_4(-\alpha(s), -\alpha(t)) = \int_0^1 du u^{-\alpha(s)-1} (1-u)^{-\alpha(t)-1} \rightarrow$$

$$B_5 = \int_0^1 \int_0^1 \frac{du_i du_j}{1-u_i u_j} u_1^{-\alpha_{12}-1} u_2^{-\alpha_{23}-1} u_3^{-\alpha_{34}-1} u_4^{-\alpha_{45}-1} u_5^{-\alpha_{51}-1}. \quad (9)$$

The variable  $u_i$  is constrained by,

$$u_i = 1 - u_{i-1} u_{i+1}, i = 1, \dots, 5, u_6 = u_1, u_0 = u_5. \quad (10)$$

Consider the process  $1 + 2 \rightarrow 3 + 4 + 5$ , it is expressed with

$$B_5 = \int_0^1 du_1 \int_0^1 du_4 u_1^{-\alpha_{12}-1} u_4^{-\alpha_{45}-1} \left(1 - \frac{u_1}{1-u_1 u_4}\right)^{-\alpha_{23}-1} (1-u_1 u_4)^{-\alpha_{15}-2}. \quad (11)$$

In the high energy limit( $s_{34}, s_{45} \rightarrow \infty$ ), by changing the variables

$$u_1 = e^{\frac{-xy}{\alpha_{34}\alpha_{45}}}, u_4 = e^{\frac{y}{\alpha_{45}}}, \quad (12)$$

the amplitude can be rewritten to

$$B_5 = (-\alpha_{34})^{\alpha_{23}} (-\alpha_{45})^{\alpha_{15}} g(K, s_{23}, s_{15}),$$

$$g(K, s_{23}, s_{15}) = (a)^{\alpha_{23}+\alpha_{15}} \int_0^\infty dx \int_0^\infty dy x^{-\alpha_{23}-1} y^{-\alpha_{15}-1} e^{-x-y+\frac{xy}{aK}}, \quad (13)$$

where  $a$  is the slope of the trajectory,  $K(x', y') = \frac{1-e^{-x'y'}}{1-e^{-x'y'-y'}} \frac{1}{x'}$  and  $x' = -x/\alpha_{23}, y' = -y/\alpha_{45}$ . It has exactly the double Regge limit behavior. Based on this double Regge limit amplitude, the authors in Ref. [7] have investigated the  $\pi^- p \rightarrow K \bar{K} n$  data. Dalitz Plots are also given by them therein.

### 2.1.2 Hopkinson's $B_5$ model

Hopkinson and Plahte start from another way to generate the  $B_4$  model[8],

$$B_N(x) = \sum_{k_{iN-1}=0}^{\infty} \left\{ \prod_{i=2}^{N-3} (-1)^{k_{iN}} \binom{z_{i,N-1}}{k_{i,N-1}} \right\} B_4(x_{N-2,N-1}, x_{N-1,N+\sum_{i=2}^{N-3} k_{iN-1}}) B_{N-1}(x'), \quad (14)$$

where  $z_{ij} = x_{ij} - x_{i+1,j} - x_{i,j-1} + x_{i+1,j-1}$  and  $x_{ij} = -\alpha_{ij}(s_{ij})$ . For  $N = 5$ , the amplitude is

$$\begin{aligned} B_5(x) &= \sum_{k=0}^{\infty} (-1)^k \binom{z_{24}}{k} B_4(x_{34}, x_{45} + k) B_4(x_{12} + k, x_{23}) \\ &= B_4(x_{34}, x_{45}) B_4(x_{12}, x_{23}) {}_3F_2(-x_{12} + x_{34} + x_{45}, x_{13}, x_{25}; x_{45} + x_{25}, x_{13} + x_{34}; 1), \end{aligned} \quad (15)$$

where

$${}_3F_2(a, b, c; d, e; z) = \sum_{k=0}^{\infty} \frac{\Gamma(a+k)\Gamma(b+k)\Gamma(c+k)\Gamma(d)\Gamma(e)}{\Gamma(a)\Gamma(b)\Gamma(e)\Gamma(d+k)\Gamma(e+k)} \frac{z^k}{k!}.$$

Bialas and Pokorski[9] investigated the double Regge limit and the single reggelimit from Eq. (15). The  $a + b \rightarrow 1 + 2 + 3$  is used by them, and the amplitude is

$$B_5 = B_4(12, A1) B_4(23, B3) {}_3F_2(-AB + 12 + 23, A1, B3; 12 + A1, 23 + B3), \quad (16)$$

where  $A1 = -\alpha_{A1}$ , and so on.

When  $s_{12}$  and  $s_{23}$  is large, the amplitude shows a double Regge limit,

$$B_5 = B_4(AB, A1) B_4(23, B3 - A1) + B_4(AB, B3) B_4(12, A1 - B3), \quad (17)$$

and in the very high energy region of  $s_{12}$  and  $s_{23}$ , the amplitude is approximate to

$$B_5 = B_4(12, A1) B_4(23, B3). \quad (18)$$

The single Regge limit is given when  $s_{12}$  or  $s_{23}$  goes large, for example when  $s_{23}$  is fixed, the amplitude is

$$\begin{aligned} B_5 &= B_4(AB, A1) R_{23}, \\ R_{23} &= \sum_{m=0}^{\infty} \frac{1}{23+m} \frac{(-1)^m}{m!} \frac{\Gamma(B3)}{\Gamma(B3-m)} F(A1, -m; B3-m; \frac{13}{AB}). \end{aligned} \quad (19)$$

Jones and Wyld[10] have examined the single Regge limit with the above equation to  $\bar{p}n \rightarrow 3\pi$ . However, the result shows that the amplitude did not match the data very well.

## 2.2 The connection between single regge limit and the double regge limit(Dec 17 ,2013)

Bialas and Pokorski investigated the double Regge limit and the single regge limit. The  $a + b \rightarrow 1 + 2 + 3$  is used by them, and the double Regge limit amplitude Fig. 7(d) is

$$B_5 = B_4(AB, A1)B_4(23, B3 - A1) + B_4(AB, B3)B_4(12, A1 - B3), \quad (20)$$

and in the high energy region of  $s_{12}$  and  $s_{23}$ , the amplitude should be

$$B_5 \sim B_4(12, A1)B_4(23, B3) \sim (12)^{-A1}(23)^{-B3}\Gamma(A1)\Gamma(B3), \quad (21)$$

where  $A1 = -\alpha_{A1}$ , and  $B3 = -\alpha_{B3}$ .

The single Regge limit is given when  $s_{12}$  or  $s_{23}$  goes to large energy, for example when  $s_{23}$  is fixed Fig. 7(b), the amplitude is

$$B_5 = B_4(AB, A1)B_4(23, B3 - A1)F(A1, 23; 1 + A1 - B3; \frac{12}{AB}) \quad (22)$$

$$+ B_4(AB, B3)B_4(12, A1 - B3)F(B3, 23 + B3 - A1; 1 + B3 - A1; \frac{12}{AB}),$$

$$= B_4(AB, A1)B_4(23, B3)F(A1, 23; B3 + 23; \frac{13}{AB}). \quad (23)$$

We can prove that when  $s_{12}$  and  $s_{23}$  go to large area, this single regge limit can become double regge limit.

$$B_5 \rightarrow B_4(AB, A1)B_4(23, B3 - A1)F(A1; 1 + A1 - B3; \frac{12 \cdot 23}{AB}) \quad (24)$$

$$+ B_4(AB, B3)B_4(12, A1 - B3)F(B3; 1 + B3 - A1; \frac{12 \cdot 23}{AB})$$

$$\rightarrow \Gamma(A1)(AB)^{-A1}\Gamma(B3 - A1)(23)^{A1-B3}\frac{\Gamma(1 + A1 - B3)}{\Gamma(1 - B3)}(k)^{-A1}$$

$$+ \Gamma(B3)(AB)^{-B3}\Gamma(A1 - B3)(12)^{B3-A1}\frac{\Gamma(1 + B3 - A1)}{\Gamma(1 - A1)}(k)^{-B3}$$

$$\sim \Gamma(A1)\Gamma(B3)(12)^{-A1}(23)^{-B3},$$

where  $k = \frac{12 \cdot 23}{AB}$  and  $F(a, c, z) \xrightarrow{z \rightarrow -\infty} \frac{\Gamma(c)}{\Gamma(c-a)}(-z)^{-A}$  are used.

## 2.3 The phase space of five particles interaction(Nov 27 ,2013)

For  $a + b \rightarrow 1 + 2 + 3$  system, the distribution of  $s_{12}$  and  $s_{23}$  is given by[7]:

$$\frac{d^2\sigma}{ds_{12}ds_{23}} = \frac{1}{(4\pi)^2\lambda(s, m_a^2, m_b^2)} \int \int \frac{dt_{a1}dt_{b3}}{\sqrt{-\Delta_4}} |A(s_{12}, s_{23}, t_{a1}, t_{b3})|^2, \quad (25)$$

where  $\lambda(s, m_a^2, m_b^2)$  is

$$\lambda(x, y, z) = x^2 + y^2 + z^2 - 2xy - 2yz - 2zx, \quad (26)$$

and  $\Delta_4$  is the symmetric determinant with

$$\Delta_4 = \begin{vmatrix} m_b^2 & \frac{1}{2}(s - m_a^2 - m_b^2) & \frac{1}{2}(-t_{a1} + m_a^2 + m_1^2) & \frac{1}{2}(s - s_{12} + t_{b3} - m_b^2) \\ \frac{1}{2}(s - m_a^2 - m_b^2) & m_b^2 & \frac{1}{2}(s - s_{23} + t_{a1} - m_a^2) & \frac{1}{2}(-t_{b3} + m_a^2 + m_3^2) \\ \frac{1}{2}(-t_{a1} + m_a^2 + m_1^2) & \frac{1}{2}(s - s_{23} + t_{a1} - m_a^2) & m_1^2 & \frac{1}{2}(s - s_{12} - s_{23} + m_2^2) \\ \frac{1}{2}(s - s_{12} + t_{b3} - m_b^2) & \frac{1}{2}(-t_{b3} + m_a^2 + m_3^2) & \frac{1}{2}(s - s_{12} - s_{23} + m_2^2) & m_3^2 \end{vmatrix}, \quad (27)$$

which give the boundary of the  $s_{12}, s_{23}, t_{a1}$  and  $t_{b3}$ [11]. With fixed  $t_{a1}$  and  $t_{b3}$ , we can have the Dalitz plot of  $s_{12}$  and  $s_{23}$ .

## 2.4 Dalitz Plots of the $B_5$ model(Nov 22 ,2013)

Here we try to use the two different amplitudes from the above section to investigate the single and double Regge limits of the  $\gamma P \rightarrow K^+ K^- P$  process. One is the Hopkinson's amplitude, and the other one is Chan Hong-Mo's amplitude in Ref. [7] which is a modified Ruegg's amplitude.

The intermediated states are chosen to be  $\rho, K^*$  and  $\Sigma$ , and the masses of them are  $m_p = 0.983\text{GeV}$ ,  $m_K = 0.493\text{GeV}$ ,  $m_\gamma = 0\text{GeV}$ . The trajectories are chosen to be

$$\begin{aligned} \alpha_{t_{b3}} &= 0.483 + 0.885s + 0.1i, \quad \alpha_{t_{a1}} = 0.3 + 1.0s + 0.12i, \\ \alpha_{s_{ab}} &= 0.5 + 0.9si, \quad \alpha_{s_{12}} = 0.5 + 0.9s + 0.05i, \quad \alpha_{s_{23}} = -0.2 + 0.9s + 0.23i \end{aligned} \quad (28)$$

$s_{ab}$  is fixed to be  $20.1\text{GeV}^2$ . The Dalitz Plots are shown in Fig. 1.

## 2.5 Generalized B5 model with kinematic factors(Nov 27 ,2013)

When the interaction includes baryons, there always has a kinematic factors. The amplitude of five-point function with  $\pi^- P \rightarrow K^0 \bar{K}^- P$  in Fig. 6 generally has the following structure[12, 13, 14], when the intermediate states are spin-1 mesons or P-wave baryons.

$$A = c \cdot \epsilon_{\mu\nu\rho\sigma} p_\pi^\mu p_K^\nu p_K^\rho p_P^\sigma \times B_5(1 - \alpha_{K^*}, 1 - \alpha_A, \frac{3}{2} - \alpha_{Y^*}, 1 - \alpha_\omega, \frac{3}{2} - \alpha_\Delta), \quad (29)$$

where  $c$  is a normalization constant.

For a photoproduction case in Fig. 7(a), the amplitude should be:

$$\mathcal{A} = c \cdot \epsilon_{\mu\nu\rho\sigma} \varepsilon^\mu p_K^\nu p_{K^-}^\rho p_P^\sigma \times B_5(1 - \alpha_{K^*}, 1 - \alpha_A, \frac{3}{2} - \alpha_{Y^*}, 1 - \alpha_\omega, \frac{3}{2} - \alpha_{N^*}), \quad (30)$$

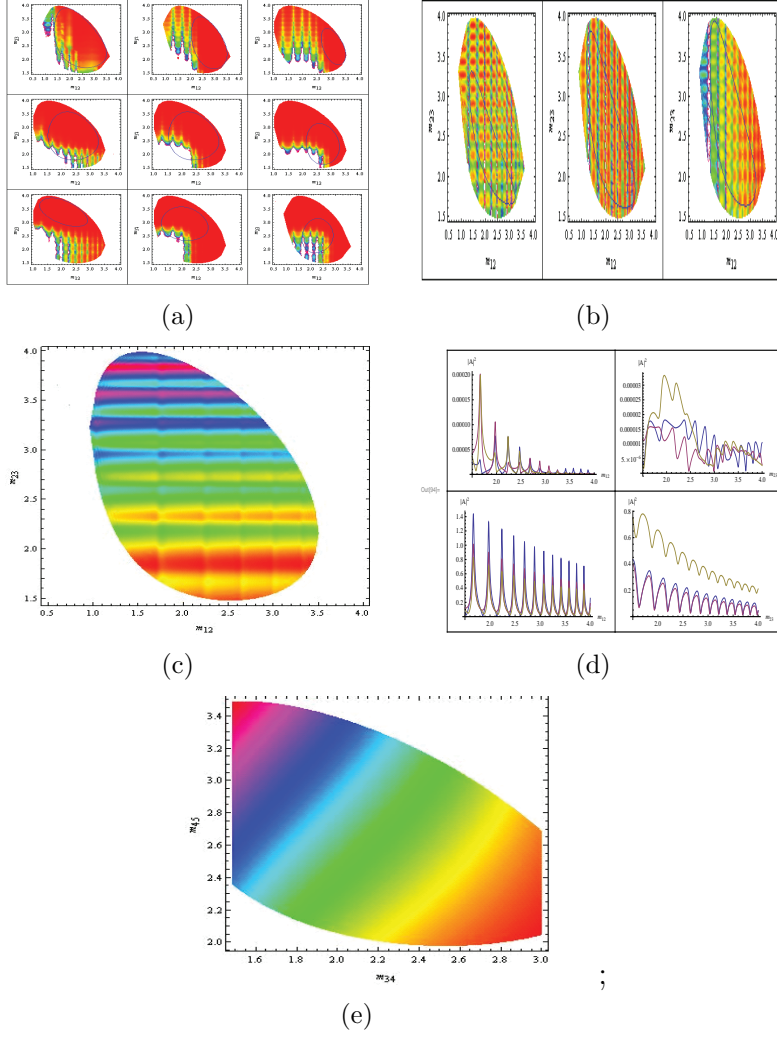
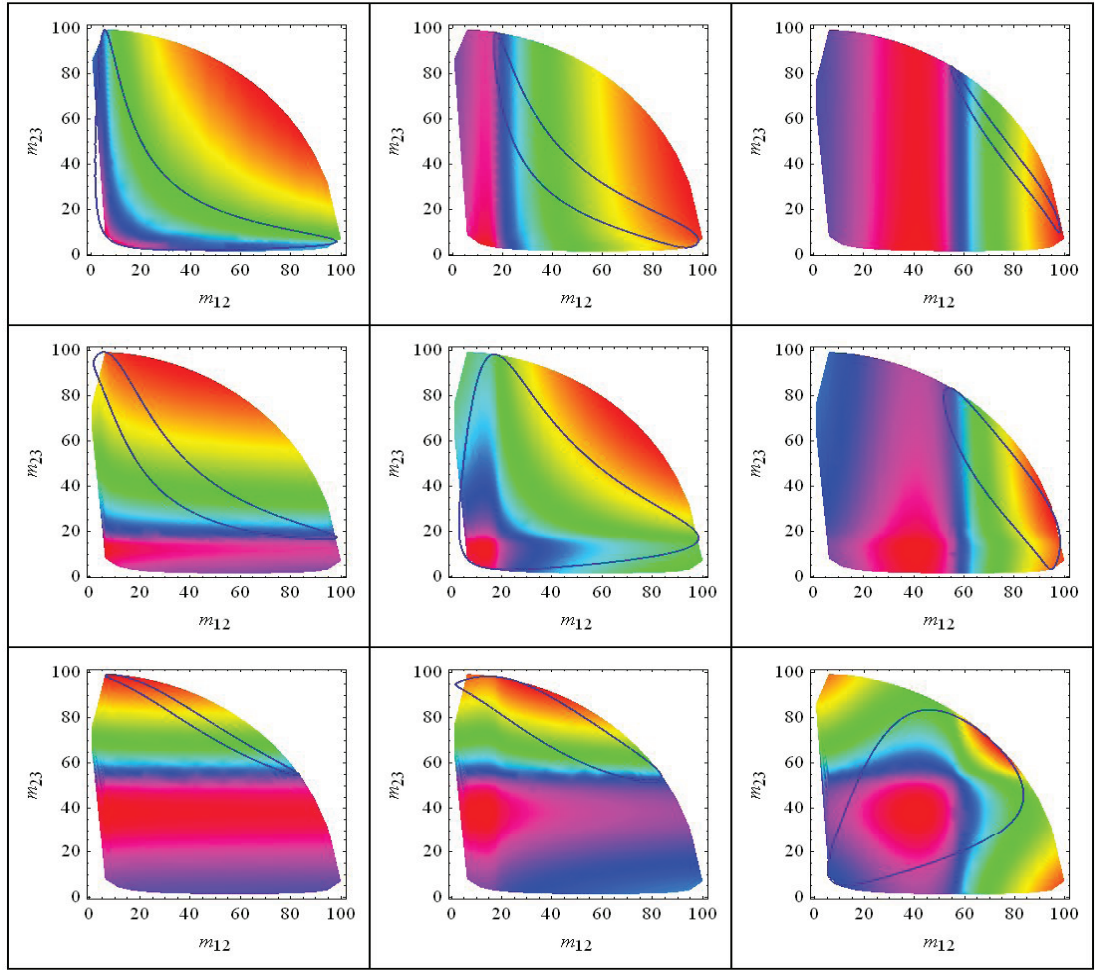
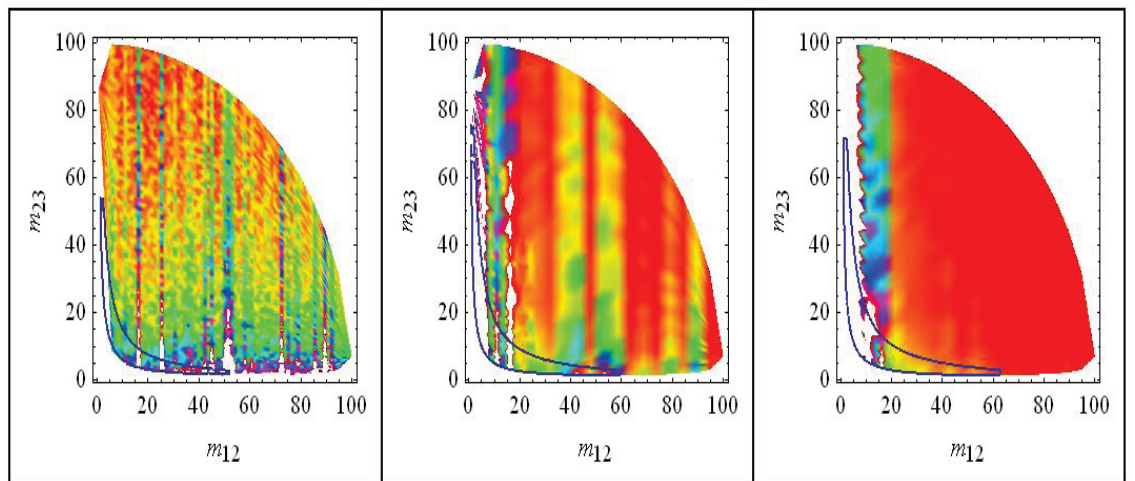


Figure 1: (a), (b) the double Regge limits of Eq. 20, (a) with  $t_1 = \{-3, -6, -9\}$ ,  $t_2 = \{-3, -6, -9\}$ , (b) small  $t_1, t_2$ ,  $t_1 = -0.8$  and  $t_2 = -1.4$ . The blue circle in the plot is the real boundary of  $m_{12}$  and  $m_{23}$ . (c) the double Regge limits of Eq. 18 ( $t_1 = t_2 = -6$ ) (d), the single Regge limit of Eq. 22 with fixed  $s_{23}$  (left) and fixed  $s_{12}$  (right), and  $t_1 = -6 = t_2 = -6$  (up);  $t_1 = -0.3, -0.8, -1.4$ ,  $t_2 = -0.8$  (down); (e), the double Regge limits from the Ref.[7] (Logarithmic Plot).



(a)

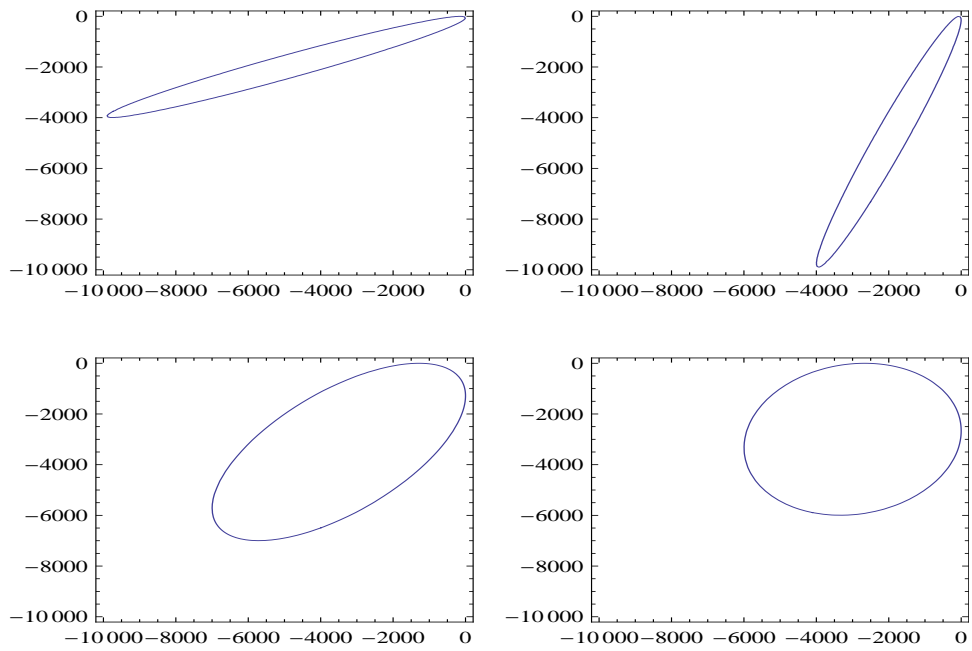


8

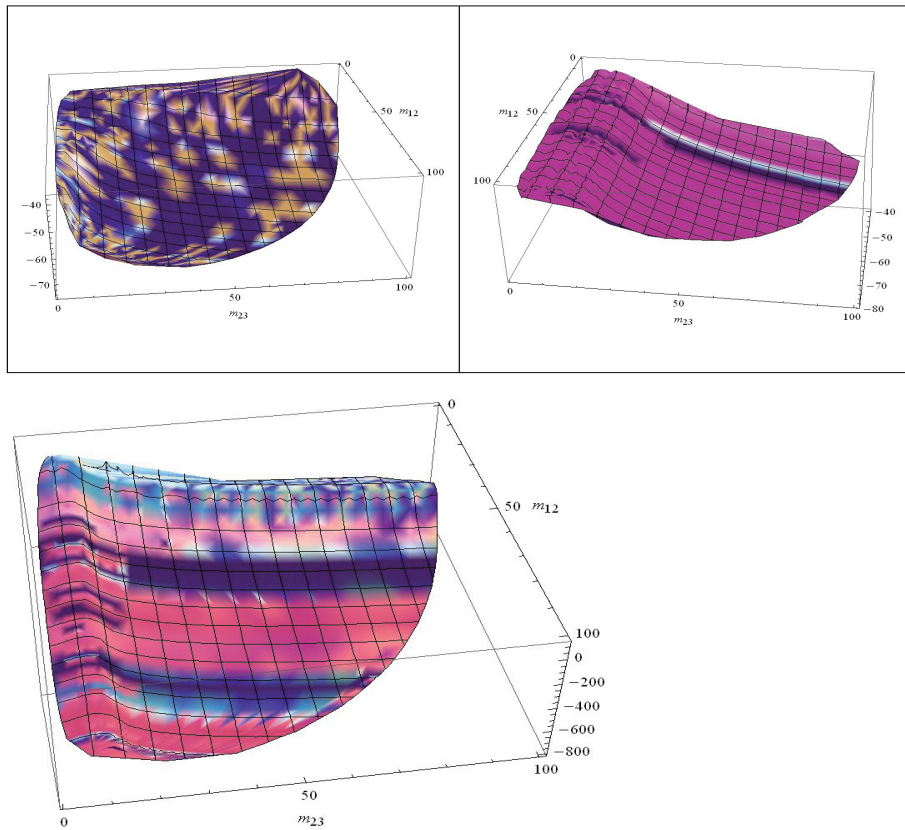
(b)

Figure 2: a, the double Regge limit with larger region,  $sab = 10000$ ,  $t_1 = -30, -300, -3000$ ,  $t_2 = -30, -300, -3000$ ; b)the double Regge limits with larger region,  $sab = 10000$ ,  $t_1 = -0.3, -0.8, -1.4$ ,  $t_2 = -0.8$ .





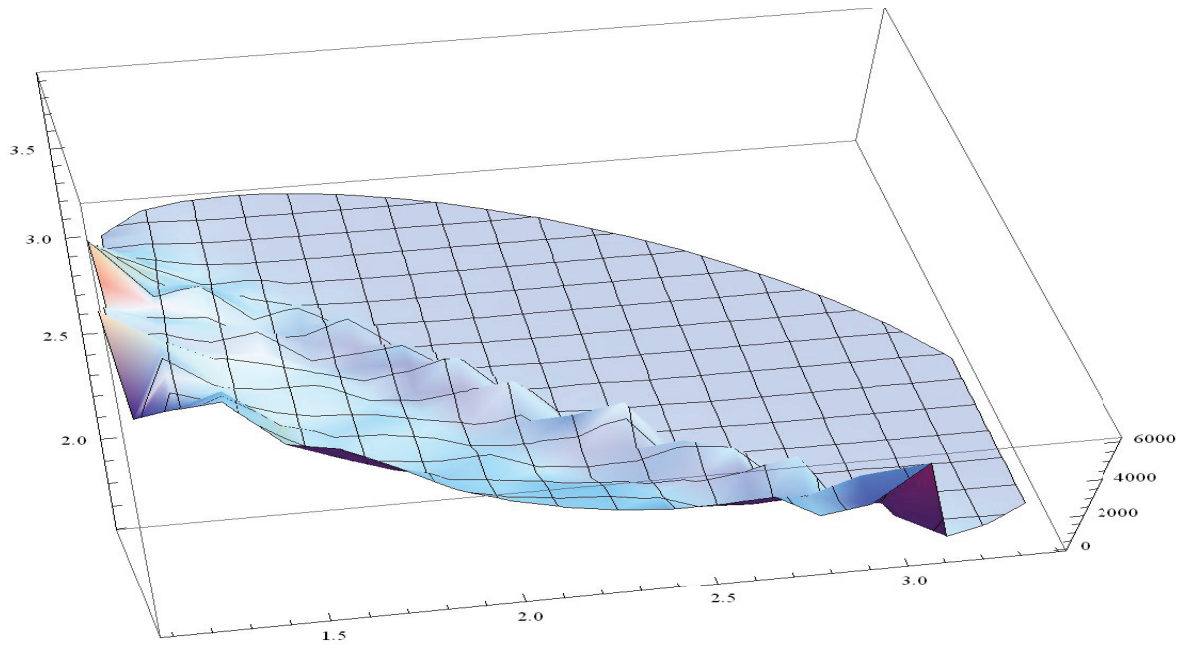
(a)



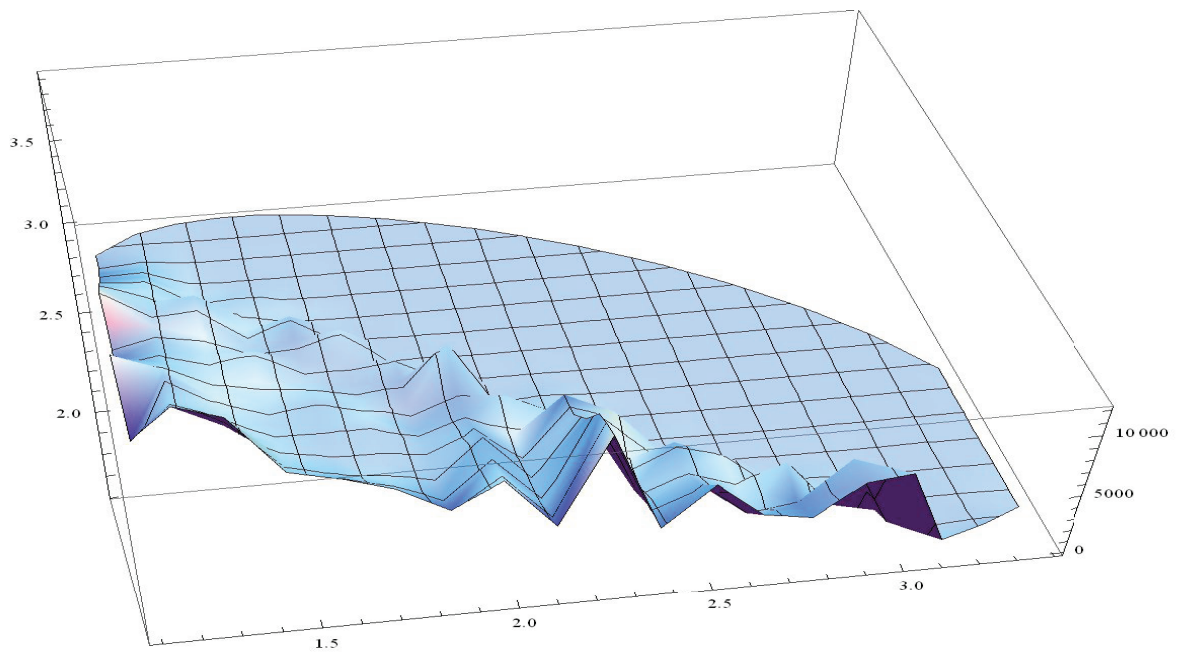
9

(b)

Figure 3: a), Boundary of  $t_{b3}$  and  $t_{a1}$ ,  $t_1 = 6000, 10, 3000, 4000, t_2 = 10, 6000, 3000, 4000$ ; b), The behavior of single regge and double regge limits: they have the same behavior at the central region.



(a)



(b)

Figure 4: The Dalitz Plots by Fortran code: a),the single regge limit with fixed  $s_{23}$ ; b)the single regge limit with fixed  $s_{12}$ .

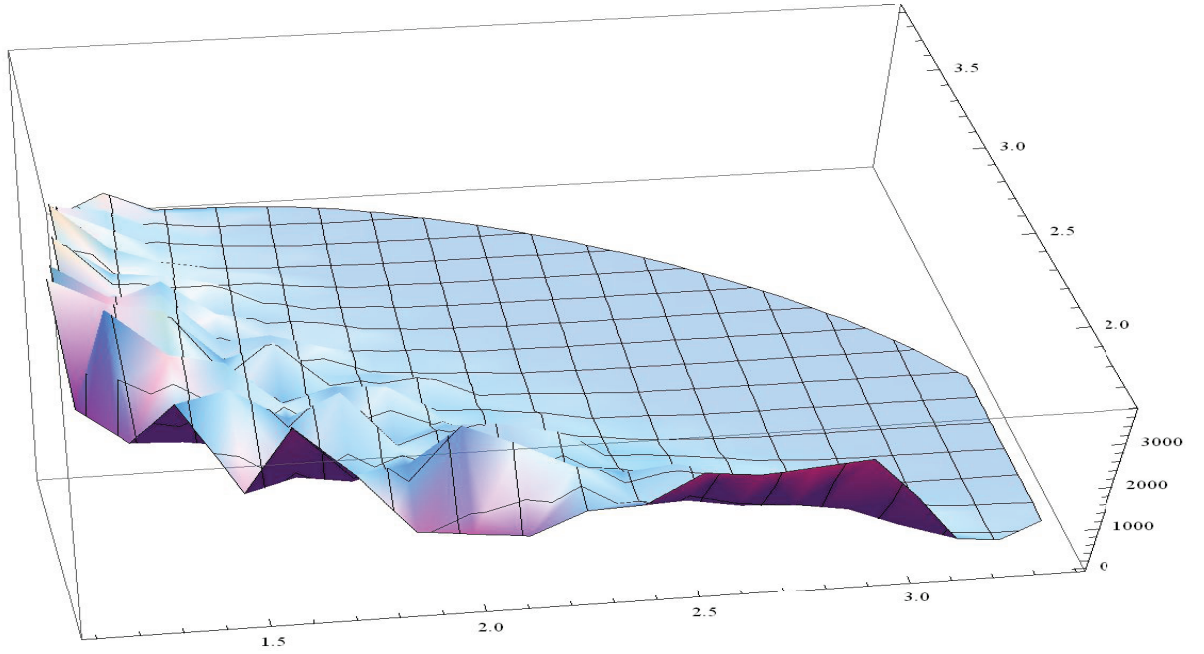


Figure 5: The Dalitz Plots by Fortran code: a), the double Regge limit

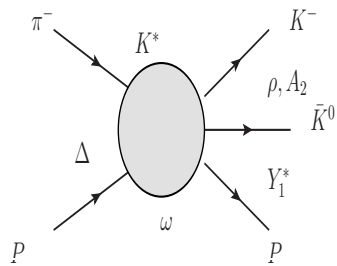


Figure 6:  $\pi P \rightarrow K^- \bar{K}^0 P$

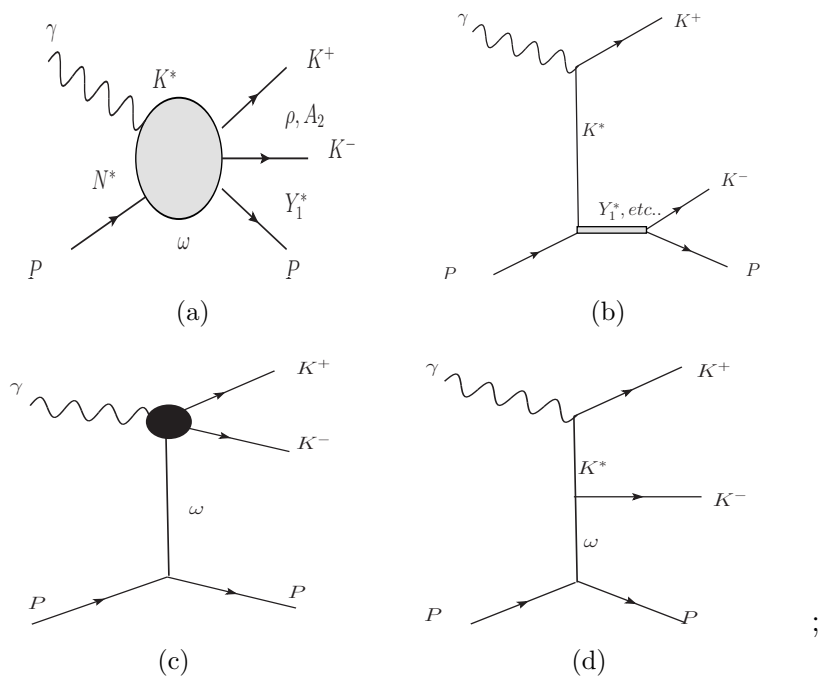


Figure 7: a, a general diagram of  $\gamma P \rightarrow K^+ K^- P$ ; b,c,d, including the particular intermediate states in each diagram.

where  $\varepsilon^\mu$  is the polarization vector of the photon. One only needs to change the  $\pi^\mu$  to the photon polarization vector  $\varepsilon^\mu$  since the intermediate states are same as  $\pi$  production.

The case of Fig. 7(b), Fig. 7(c) and Fig. 7(d) are the single Regge limits and the double Regge limit, which correspond different energy regions of the Dilatz Plot. The relation between them are still being researched.

## References

- [1] G. Veneziano. Nuovo Cimento **57A** (1968) 190.
- [2] C. Lovelce. Physics Letters **28**(1968) 264.
- [3] J. A. Shapiro. Physical Review **179**(1969) 1345.
- [4] S. Pokorski, R. O. Raitio, G. H. Thomas. Il Nuovo Cimento A Series 11 **7** (1972) 828.
- [5] D. Sivers, J. Yellin. Review of Modern Physics **43** (1971)125.
- [6] K. Bardakci, H. Ruegg. Physics Letters B **28**(1968) 342.
- [7] Chan Hong-Mo, K. Kajantie, G. Ranft. IL Nuovo Cimento. ILA (1967) 157.
- [8] J. F. L. Hopkinson, E. Plahte. Physics Letters B **28** (1969)489.
- [9] A. Bialas, S. Pokorski. Nuclear Physics B **10** (1969) 399.
- [10] L. Jones, H. Wyld. Phys. Rev. Letters **23**(1969)814.
- [11] P. Nyborg, H. S. Song, et al.. Physics Review **140**(1965)914.
- [12] J. Bartsch, et al.. Nuclear Physics B **23** (1970)1.
- [13] B. Petersson, N. A. Törnqvist. Nuclear Physics B **13** (1969)629.
- [14] Chan Hong-Mo, et al.. Nuclear Physics B **19** (1970)173.
- [15] D. K. CAMPBELL, D. I. OLIVE and W. J. ZAKRZEWSKI. Nuclear Physics B **14**(1969) 319.